Maneuvering Angle Rigid Formations With Global Convergence Guarantees

Liangming Chen, Zhiyun Lin, *Senior Member, IEEE*, Hector Garcia de Marina, *Member, IEEE*, Zhiyong Sun, and Mir Feroskhan

***Abstract*—Angle rigid multi-agent formations can simultaneously undergo translational, rotational, and scaling maneuvering, therefore combining the maneuvering capabilities of both distance and bearing rigid formations. However, maneuvering angle rigid formations in 2D or 3D with global convergence guarantees is shown to be a challenging problem in the existing literature even when relative position measurements are available. Motivated by angle-induced linear equations in 2D triangles and 3D tetrahedra, this paper aims to solve this challenging problem in both 2D and 3D under a leader-follower framework. For the 2D case where the leaders have constant velocities, by using *local* relative position and velocity measurements, a formation maneuvering law is designed for the followers governed by double-integrator dynamics. When the leaders have time-varying velocities, a sliding mode formation maneuvering law is proposed by using the same measurements. For the 3D case, to establish an angle-induced linear equation for each tetrahedron, we assume that all the followers' coordinate frames share a common *Z* direction. Then, a formation maneuvering law is proposed for the followers to globally maneuver *Z-weakly* angle rigid formations in 3D. The extension to Lagrangian agent dynamics and the construction of the desired rigid formations by using the minimum number of angle constraints are also discussed. Simulation examples are provided to validate the effectiveness of the proposed algorithms.**

***Index Terms*—Angle rigid formations, formation control, formation maneuvering, global convergence, multi-agent systems.**

I. Introduction

MULTI-AGENT formations have been extensively studied [1] to enable numerous impactful applications, such as target search and rescue [2], unknown environment exploration [3], and cooperative surveillance [4]. In most of these practical applications, the agents are required to have the capability of not only achieving a specific formation shape, but also maneuvering collectively as a whole in translation, rotation, scaling, and with even more complicated motion forms [5]–[12].

To achieve the aforementioned formation maneuvering task, various control approaches have been proposed, which can be categorized into different types according to the constraints used to specify the desired formation shape [7], [13], [14]. For relative position-constrained formations [15]–[17], since the inter-agent relative positions are invariant when the associated agents translate with the same magnitude, translational formation maneuvering can be achieved, assuming that the agents' coordinate frames are aligned. Since inter-agent distances are invariant under the agents' translation and rotation, both translational and rotational formation maneuvering are achieved for distance rigid formations [18]. Also, since inter-agent bearings are invariant under the agents' translational and scaling motions [13], both translational and scaling formation maneuvering are achieved for bearing rigid formations [13], [19], [20], where the results hold for an arbitrary dimensional space provided that the agents' coordinate frames are aligned. Under a leader-follower framework, the bearing-constrained formation tracking problem has been investigated in [21], [22], where the translational formation maneuvering is achieved by using relative position and absolute velocity measurements. Unlike the distance and bearing rigid formations alone, angle rigid formations can undergo simultaneously translational, rotational and scaling maneuvering because any angle constraints are invariant under these three types of formation maneuvering motions [7], [23], [24]. With the advantage of having more formation maneuvering freedoms, angle rigid formation maneuvering algorithms have been designed in [7] for single-integrator agents, and in [25] for double-integrator agents. However, their convergence to their respective desired formations under the designed formation maneuvering algorithms [7], [25] is only locally guaranteed. Due to the high nonlinearity in the angle rigid formations' closed-loop dynamics, it is challenging to determine the attraction region of the locally convergent formations [1], [26].

Motivated by the aforementioned drawbacks, we aim to achieve the formation maneuvering of angle rigid formations with global convergence, where the agents can have their own local coordinate frames, and the maneuvering motions include translation, rotation and scaling. Different from the maneu-

Manuscript received April 25, 2022; accepted May 18, 2022. The work of Z. Lin was supported by National Natural Science Foundation of China (62173118). The work of H. Garcia de Marina was supported by the *Ramon y Cajal* (RYC2020-030090-I) from the Spanish Ministry of Science. Recommended by Associate Editor Xiaohua Ge. *(Corresponding author: Zhiyun Lin and Mir Feroskhan.)*

Citation: L. Chen, Z. Lin, H. Garcia de Marina, Z. Sun, and M. Feroskhan, "Maneuvering angle rigid formations with global convergence guarantees," *IEEE/CAA J. Autom. Sinica*, vol. 9, no. 8, pp. 1464–1475, Aug. 2022.

L. Chen and M. Feroskhan are with the School of Mechanical and Aerospace Engineering, Nanyang Technological University, Singapore 639798, Singapore (e-mail: liangming.chen@ntu.edu.sg; mir.feroskhan@ntu.edu.sg).

Z. Lin is with the Department of Electrical and Electronic Engineering, Southern University of Science and Technology, Shenzhen 518055, China (e-mail: linzy@sustech.edu.cn).

H. Garcia de Marina is with the Department of Computer Architecture and Technology, and also with CITIC, University of Granada, 18014 Granada, Spain (e-mail: hgarciad@ucm.es).

Z. Sun is with the Department of Electrical Engineering, Eindhoven University of Technology, 5600 MB Eindhoven, the Netherlands (e-mail: z.sun@tue.nl).

Color versions of one or more of the figures in this paper are available online at http://ieeexplore.ieee.org.

Digital Object Identifier 10.1109/JAS.2022.105749

vering approaches in [7], [25], [27], we employ angle-induced linear equations in 2D triangles and 3D tetrahedra to design *linear* formation maneuvering laws in 2D and 3D, respectively. We consider that the agents are governed by double-integrator dynamics and the available sensor measurements are relative positions and velocities. Compared with the existing results, the main contributions of this paper are summarized as follows:

1) Compared with relative position-constrained, distance-constrained and bearing-constrained formation maneuvering approaches, the proposed angle-constrained formation maneuvering laws enable the maneuvering motions of simultaneous translation, rotation and scaling. Compared with relative position-constrained and bearing-constrained formations which require agents to have aligned coordinate frames, angle rigid formations allow agents to have non-aligned local coordinate frames.

2) Compared with the existing 2D angle-constrained formation maneuvering laws guaranteeing local convergence [7], [25] and angle-constrained flocking law guaranteeing almost global convergence [27], both of our proposed 2D and 3D angle-constrained formation maneuvering laws have global convergence guarantees.

3) Although both the angle-displacement [8] and affine [5], [28], [29] formation maneuvering approaches enable the maneuvering motions of simultaneous translation, rotation and scaling, the number of leaders required for maneuvering motion control in these works is higher than that of our work which only requires 2 leaders in both 2D and 3D cases. Specifically, the number of leaders should be at least 3 for the algorithms in [5], [29] in 2D, while at least 4 for the algorithms in [5], [8], [29] in 3D.

The rest of the paper is organized as follows. Section II presents the preliminary findings. Sections III and IV introduce the maneuvering strategies of angle rigid formations in 2D and 3D, respectively. Some discussion is conducted in Section V. Simulation results are provided in Section VI.

II. Preliminaries

A. Notations

We consider a multi-agent system consisting of $N \geq d+1$ mobile agents in $\mathbb{R}^d$ space, where $d = 2,3$ represent the cases of 2D plane and 3D space, respectively. Let $\mathcal{V} = \{1,2,\ldots,N\}$ be the set of the agents which are labeled from 1 to N. The agents' positions are denoted by $p = [p_1^\top, p_2^\top, \ldots, p_N^\top]^\top \in \mathbb{R}^{dN}$, where agent i' s position is $p_i \in \mathbb{R}^d$. Let I_N, 1_N, $\otimes$ $\lambda_{\max}$, $\lambda_{\min}$, det() be the N-by-N identity matrix, $N \times 1$ column vector of all ones, the Kronecker product, the maximum eigenvalue, the minimum eigenvalue of a real-valued symmetric matrix, and the determinant of a square matrix, respectively. Let $R(\theta) \in SO(2)$ be the 2D rotation matrix with rotation angle $\theta \in [0, 2\pi)$. Let $R_x(\theta) \in SO(3), R_y(\phi) \in SO(3)$ and $R_z(\varphi) \in SO(3)$ be the 3D rotation matrices along the X, Y and Z axes with rotation angles $\theta \in \mathbb{R}, \phi \in \mathbb{R}$ and $\varphi \in \mathbb{R}$, respectively. In this paper, we assume that each agent holds an unknown but fixed coordinate frame $\sum_i$ to conduct relative measurements regarding its neighbors. We define $\sum_g$ as the global coordinate frame. In 2D, let $R_g^i \in SO(2)$ be the 2D rotation matrix describing the rotation from $\sum_g$ to $\sum_i$.

B. Angle Rigid Formations

As introduced in [23], since each interior angle is associated with three vertices, we use the notion of *angularity* instead of a graph to describe multi-agent formations with angle constraints. For the vertex set $\mathcal{V} = \{1,2,\ldots,N\}$, define a three-vertex *triplet* (i,j,k) to describe the angle constraint $\measuredangle ijk$ between the rays $\overrightarrow{ji}$ and $\overrightarrow{jk}$. Then, we define $\mathcal{A} \subseteq \mathcal{V}\times\mathcal{V}\times\mathcal{V} = \{(i,j,k), i,j,k \in \mathcal{V}, i \neq j \neq k\}$ as an angle set, of which each element is a triplet. Because constraining $\measuredangle ijk$ is equivalent to constraining $\measuredangle kji$, the notation of the triplet (i,j,k) is equivalent to (k,j,i). The combination of the vertex set $\mathcal{V}$, the angle set $\mathcal{A}$ and the position configuration $p \in \mathbb{R}^{dN}$ is called an *angularity* which we denote by $\mathbb{A}(\mathcal{V},\mathcal{A},p)$. If $(i,j,k) \in \mathcal{A}$, then $\{j,k\} \in \mathcal{N}_i, \{i,k\} \in \mathcal{N}_j, \{i,j\} \in \mathcal{N}_k$ where $\mathcal{N}_i$ represents agent i' s neighbor set. Two angularities $\mathbb{A}(\mathcal{V},\mathcal{A},p)$ and $\mathbb{A}'(\mathcal{V},\mathcal{A},p')$ are said to be *equivalent* if their corresponding angles defined in $\mathcal{A}$ have the same magnitude, and said to be *congruent* if all possible angles formed by three vertices of $\mathcal{V}$ have the same magnitude [23]. Then, angle rigidity of angularities is formally defined as follows.

Definition 1 [23]: An angularity $\mathbb{A}(\mathcal{V},\mathcal{A},p)$ is angle rigid if there exists an $\epsilon > 0$ such that every angularity $\mathbb{A}'(\mathcal{V},\mathcal{A},p')$ that is equivalent to $\mathbb{A}(\mathcal{V},\mathcal{A},p)$ and satisfies $\|p'-p\| < \epsilon$ is also congruent to $\mathbb{A}(\mathcal{V},\mathcal{A},p)$. We say $\mathbb{A}$ is globally angle rigid if every angularity that is equivalent to it is also congruent to it.

We say $\mathcal{A}$ is a *triangular angle set* if for every $(i_1,j_1,k_1) \in \mathcal{A}$, there also exists $\{(j_1,k_1,i_1),(k_1,i_1,j_1)\} \subseteq \mathcal{A}$ [30]. Then, a triangular angle set $\mathcal{A}$ can be written in the form of

$$\mathcal{A} = \{\ldots,(i_1,j_1,k_1),(j_1,k_1,i_1),(k_1,i_1,j_1),\ldots\} \tag{1}$$

and $\mathcal{S}_{\triangle i_1 j_1 k_1} = \{(i_1,j_1,k_1),(j_1,k_1,i_1),(k_1,i_1,j_1)\}$ is denoted by the triangular angle set of $\triangle i_1 j_1 k_1$. We say $\mathbb{A}(\mathcal{V},\mathcal{A},p)$ is a *triangular angularity* if $\mathcal{A}$ is a triangular angle set. The number of triangles in the triangular angularity $\mathbb{A}(\mathcal{V},\mathcal{A},p)$ is denoted by $n_{\mathcal{A}}^{\triangle} \in \mathbb{N}^+$. Then, we say $\mathcal{A}$ is a *tetrahedral angle set* if $\mathcal{A}$ is a triangular angle set and for every triangular angle subset $\mathcal{S}_{\triangle i_1 j_1 k_1} \in \mathcal{A}$, there always exists a vertex $m \in \mathcal{V}$, $m \neq i \neq j \neq k$ such that $\mathcal{S}_{\triangle i_1 j_1 m} \in \mathcal{A}$, $\mathcal{S}_{\triangle i_1 k_1 m} \in \mathcal{A}$, $\mathcal{S}_{\triangle j_1 k_1 m} \in \mathcal{A}$. Then, a tetrahedral angle set $\mathcal{A}$ can be written in the form of

$$\mathcal{A} = \{\ldots,\mathcal{S}_{\triangle i_1 j_1 k_1},\mathcal{S}_{\triangle i_1 j_1 m},\mathcal{S}_{\triangle i_1 k_1 m},\mathcal{S}_{\triangle j_1 k_1 m},\ldots\} \tag{2}$$

and we denote the corresponding tetrahedral angle set of $\triangle\!\!\!\triangle i_1 j_1 k_1 m$ as $\mathcal{S}_{\triangle\!\!\!\triangle i_1 j_1 k_1 m} = \{\mathcal{S}_{\triangle i_1 j_1 k_1},\mathcal{S}_{\triangle i_1 j_1 m},\mathcal{S}_{\triangle i_1 k_1 m},\mathcal{S}_{\triangle j_1 k_1 m}\}$. We say $\mathbb{A}(\mathcal{V},\mathcal{A},p)$ is a *tetrahedral angularity* if $\mathcal{A}$ is a tetrahedral angle set. Denote by $n_{\mathcal{A}}^{\triangle\!\!\!\triangle} \in \mathbb{N}^+$ the total number of tetrahedra in the tetrahedral angularity $\mathbb{A}(\mathcal{V},\mathcal{A},p)$.

We say that a multi-agent formation is angle rigid if its corresponding angularity $\mathbb{A}(\mathcal{V},\mathcal{A},p)$ is angle rigid. The desired angle rigid formation is described by a set of angle constraints

$$f_{\mathcal{A}}(\alpha^*) := [\ldots,\alpha_{kij}^*,\ldots]^\top \in \mathbb{R}^{|\mathcal{A}|},\ (k,i,j) \in \mathcal{A} \tag{3}$$

where α_{kij}^* represents the desired angle among agents k,i,j. Note that the description of the desired formation is not related to the agents' positions, but only related to the magnitude of the desired angles among agents. In this paper, we are interested in the maneuvering of triangular formations in 2D and tetrahedral formations in 3D, respectively.

C. Problem Formulation

Consider an N-agent formation consisting of two leaders which will determine the whole formation's maneuvering motions, and $N-2$ followers which only have local relative measurements with respect to their neighbors. Without loss of generality, we assume that agents 1 and 2 are leaders, and denote by $\mathcal{V}_l=\{1,2\}, \mathcal{V}_f=\{3,\ldots,N\}$ the sets of the leaders and followers, respectively. Then, the position vector p can be partitioned by $p=[p^{l\top},p^{f\top}]^\top$, where $p^l=[p_1^\top,p_2^\top]^\top\in\mathbb{R}^{2d}$ and $p^f=[p_3^\top,\ldots,p_N^\top]^\top\in\mathbb{R}^{d(N-2)}$. Then, the leaders' moving trajectories can be described by

$$p^l(t)=s(t)[I_2\otimes Q(\theta(t))]p^l(0)+1_2\otimes w(t) \tag{4}$$

where $s(t)\in\mathbb{R}, Q(\theta(t))\in SO(d)$, and $w(t)\in\mathbb{R}^d$ represent the scaling, rotational and translational maneuvering parameters, respectively, $\theta(t)\in\mathbb{R}$ when $d=2$, and $\theta(t)\in\mathbb{R}^3$ when $d=3$. We consider that the followers are governed by double-integrator dynamics

$$\dot{p}_i(t)=v_i(t),\quad \dot{v}_i(t)=u_i(t),\quad \forall i=3,\ldots,N \tag{5}$$

where v_i and u_i represent agent i's velocity and control input, respectively. We also make the following assumptions:

1) The desired angularity $\mathbb{A}(\mathcal{V},\mathcal{A},p^*)$ is angle rigid where $\mathcal{A}$ is a triangular angle set in the 2D case, $\mathcal{A}$ is a tetrahedral angle set in 3D case, and $p^*\in\mathbb{R}^{dN}$ is an arbitrary configuration that satisfies all the angle constraints defined in $f_{\mathcal{A}}(\alpha^*)$.

2) The two leaders never collide with each other.

3) For the case of constant-velocity leaders, no communication is needed among the followers, while for the case of leaders with time-varying velocities, inter-agent communication is needed. For both cases, each follower i measures relative positions and velocities regarding its neighbors $\mathcal{N}_i$.

Given the desired angles in $f_{\mathcal{A}}(\alpha^*)$ and the above three assumptions, the aim is to design $u_i(t)$ for (5) such that

$$\lim_{t\to\infty}(\alpha_{ijk}(t)-\alpha^*_{ijk})=0, \forall (i,j,k)\in\mathcal{A}. \tag{6}$$

Since the formation's translation, rotation and scale are exactly determined by the two leaders and the desired formation is angle rigid, the objective (6) indeed describes the requirement of the formation maneuvering. Since the methods of calculating the angles $\alpha_{ijk}(t)$ in the 2D and 3D cases are different, we will introduce the maneuvering of 2D formations and 3D formations in the follow-up sections, separately.

III. Maneuvering 2D Angle Rigid Formations

In this 2D case, we define the signed interior angle $\alpha_{kij}\in[0,2\pi)$ among three non-coincident agents k,i,j as

$$\alpha_{kij}:=\begin{cases}\arccos(b_{ij}^\top b_{ik}), \text{ if } b_{ij}^\top b_{ik}^\perp\geq 0\\ 2\pi-\arccos(b_{ij}^\top b_{ik}), \text{ otherwise}\end{cases} \tag{7}$$

where $b_{ij}:=\frac{p_j-p_i}{\|p_j-p_i\|}$ is the bearing from agent i to agent j, $b_{ik}^\perp:=R(\frac{\pi}{2})b_{ik}=[\begin{smallmatrix}0&-1\\1&0\end{smallmatrix}]b_{ik}$ (see [23] for more details).

A. Angle-Induced Linear Equations in Triangles

Since an angle constraint (7) is highly nonlinear with respect to agents' positions p_i,p_j and p_k, it is a challenging task to achieve (6) with a global convergence guarantee. Now, we introduce the transformation of the nonlinear angle constraints existing in triangles into linear algebraic equations, under which the nonlinear control objective (6) shall be transformed into a linear form. Taking three interior angles $\alpha_{kij},\alpha_{ijk}$ and α_{jki} from non-degenerate triangle $\triangle ijk$ as an example, according to [30], one has

$$(p_j-p_i)/\|p_j-p_i\|=R(\alpha_{kij})(p_k-p_i)/\|p_k-p_i\|. \tag{8}$$

Using the law of sines $\frac{\|p_k-p_i\|}{\|p_j-p_i\|}=\frac{\sin\alpha_{ijk}}{\sin\alpha_{jki}}$ and (8), the angle-induced linear equation in $\triangle ijk$ can be written as

$$\begin{aligned}f_i^{\triangle ijk}(\alpha,p):&=A_i^{\triangle ijk}(\alpha)p_i+A_j^{\triangle ijk}(\alpha)p_j+A_k^{\triangle ijk}(\alpha)p_k\\&=\sin\alpha_{jki}(p_i-p_k)-\sin\alpha_{ijk}R^\top(\alpha_{kij})(p_i-p_j)=0\end{aligned} \tag{9}$$

where α represents those interior angles that are associated with $\triangle ijk$, p represents the configuration of the agents, and the coefficient matrices

$$\begin{aligned}A_i^{\triangle ijk}(\alpha)&:=\left(\sin\alpha_{jki}I_2-\sin\alpha_{ijk}R^\top(\alpha_{kij})\right)\in\mathbb{R}^{2\times 2}\\A_j^{\triangle ijk}(\alpha)&:=\sin\alpha_{ijk}R^\top(\alpha_{kij})\in\mathbb{R}^{2\times 2}\\A_k^{\triangle ijk}(\alpha)&:=-\sin\alpha_{jki}I_2\in\mathbb{R}^{2\times 2}.\end{aligned} \tag{10}$$

To avoid collinearity among three neighboring agents which degrades (9), the desired configuration p^* is assumed to be generic[1], where none of the triangles defined in $\mathcal{A}$ are degenerate. For a triangular angularity $\mathbb{A}(\mathcal{V},\mathcal{A},p)$ with multiple triangles in $\mathcal{A}$, writing the corresponding angle-induced linear equations (9) from the triangular angularity into a compact form yields

$$M_{\mathcal{A}}(\alpha(p))p=0 \tag{11}$$

where $M_{\mathcal{A}}(\alpha)\in\mathbb{R}^{2n_{\mathcal{A}}^{\triangle}\times 2N}$ can be written in the form of

$$\begin{array}{c} \\ \text{1st }\triangle\\ \cdots\\ \triangle ijk\\ \cdots\\ n_A^\triangle\text{th }\triangle\end{array}\begin{array}{c}\cdots\ \text{Vertex } i\ \cdots\ \text{Vertex } j\ \cdots\ \text{Vertex } k\ \cdots\\ \begin{bmatrix}\cdots&\cdots&\cdots&\cdots&\cdots&\cdots&\cdots\\ \cdots&\cdots&\cdots&\cdots&\cdots&\cdots&\cdots\\ 0&A_i^{\triangle ijk}&0&A_j^{\triangle ijk}&0&A_k^{\triangle ijk}&0\\ \cdots&\cdots&\cdots&\cdots&\cdots&\cdots&\cdots\\ \cdots&\cdots&\cdots&\cdots&\cdots&\cdots&\cdots\end{bmatrix}\end{array} \tag{12}$$

whose row blocks are indexed by the triangles defined in the triangular angle set $\mathcal{A}$ and column blocks are indexed by the vertices (more details can be found in [30]). According to [23, Lemma 2], the maximum rank of $M_{\mathcal{A}}(\alpha)$ is $2N-4$. According to the partition of $\mathcal{V}$ into the leaders' set $\mathcal{V}_l$ and the followers' set $\mathcal{V}_f$, the matrix $M_{\mathcal{A}}(\alpha)$ can be correspondingly partitioned as $M_{\mathcal{A}}(\alpha)=[M_{\mathcal{A}}^l(\alpha),M_{\mathcal{A}}^f(\alpha)]$ where $M_{\mathcal{A}}^l(\alpha)\in\mathbb{R}^{2n_\triangle^{\mathcal{A}}\times 4}$ and $M_{\mathcal{A}}^f(\alpha)\in\mathbb{R}^{2n_\triangle^{\mathcal{A}}\times(2N-4)}$. Define

$$\mathcal{L}(\alpha):=M_{\mathcal{A}}^\top(\alpha)M_{\mathcal{A}}(\alpha)=\begin{bmatrix}\mathcal{L}_{ll}(\alpha)&\mathcal{L}_{lf}(\alpha)\\\mathcal{L}_{fl}(\alpha)&\mathcal{L}_{ff}(\alpha)\end{bmatrix}\in\mathbb{R}^{2N\times 2N} \tag{13}$$

[1] This follows the definition in [31, Section 1.2].

where $\mathcal{L}_{ll}(\alpha) = (M^l_{\mathcal{A}})^\top M^l_{\mathcal{A}} \in \mathbb{R}^{4\times 4}$, $\mathcal{L}_{lf}(\alpha) = (M^l_{\mathcal{A}})^\top M^f_{\mathcal{A}} \in \mathbb{R}^{4\times(2N-4)}$, $\mathcal{L}_{fl}(\alpha) = (M^f_{\mathcal{A}})^\top M^l_{\mathcal{A}} \in \mathbb{R}^{(2N-4)\times 4}$, and $\mathcal{L}_{ff}(\alpha) = (M^f_{\mathcal{A}})^\top M^f_{\mathcal{A}} \in \mathbb{R}^{(2N-4)\times(2N-4)}$. Then, one has the following lemma.

Lemma 1: If $\mathbb{A}^*(\mathcal{V},\mathcal{A},p^*)$ is angle rigid, then $\mathcal{L}_{fl}(\alpha^*)p^{l*} + \mathcal{L}_{ff}(\alpha^*)p^{f*} = 0$, and the matrix $\mathcal{L}_{ff}(\alpha^*)$ is positive definite.

The proof of Lemma 1 can be straightforwardly obtained by using [13, Theorem 1], [32, Theorem 4], or [8, Lemma 3].

B. Maneuvering Control for the Case of Leaders With Constant Velocities

Since the desired formation is assumed to be angle rigid, by Lemma 1, the desired positions and velocities for the followers can be determined by $p^{f*}(t) := -\mathcal{L}^{-1}_{ff}(\alpha^*)\mathcal{L}_{fl}(\alpha^*)p^l(t)$ and $v^{f*}(t) := -\mathcal{L}^{-1}_{ff}(\alpha^*)\mathcal{L}_{fl}(\alpha^*)\dot{p}^l(t)$, respectively. Then, we define the position error $\tilde{p}^f(t) := p^f(t) - p^{f*}(t)$, and the velocity error $\tilde{v}^f(t) := v^f(t) - v^{f*}(t)$. Therefore, the nonlinear control objective (6) can be equivalently transformed into the following linear form:

$$\lim_{t\to\infty} \tilde{p}^f(t) = 0, \qquad \lim_{t\to\infty} \tilde{v}^f(t) = 0. \tag{14}$$

Since each follower $i \in \mathcal{V}_f$ has no knowledge of its absolute position p_i, but can measure the relative position $p_i - p_j$ with respect to its neighbors $j \in \mathcal{N}_i$, it is still challenging to design a distributed formation maneuvering algorithm to achieve (14).

Now, we design the formation maneuvering law for the followers in the compact form as

$$\begin{aligned} u^f(t) = &-k_p\left[\mathcal{L}_{ff}(\alpha^*)p^f(t) + \mathcal{L}_{fl}(\alpha^*)p^l(t)\right] \\ &-k_v\left[\mathcal{L}_{ff}(\alpha^*)v^f(t) + \mathcal{L}_{fl}(\alpha^*)v^l(t)\right] \end{aligned} \tag{15}$$

where $k_p > 0, k_v > 0$ are the position and velocity feedback gains, respectively, and $u^f(t) = [u_3^\top, \ldots, u_N^\top]^\top \in \mathbb{R}^{2N-4}$. According to (13), the component form of the formation maneuvering law (15) can be written as

$$\begin{aligned} u_i(t) = &-k_p\Bigg[\sum_{(i,j_1,k_1)\in\bar{\mathcal{A}}} (A_i^{\triangle ij_1k_1}(\alpha^*))^\top f_i^{\triangle ij_1k_1}(\alpha^*,p(t)) \\ &+ \sum_{(j_2,i,k_2)\in\bar{\mathcal{A}}} (A_i^{\triangle j_2ik_2}(\alpha^*))^\top f_i^{\triangle j_2ik_2}(\alpha^*,p(t)) \\ &+ \sum_{(j_3,k_3,i)\in\bar{\mathcal{A}}} (A_i^{\triangle j_3k_3i}(\alpha^*))^\top f_i^{\triangle j_3k_3i}(\alpha^*,p(t))\Bigg] \\ &-k_v\Bigg[\sum_{(i,j_1,k_1)\in\bar{\mathcal{A}}} (A_i^{\triangle ij_1k_1}(\alpha^*))^\top f_i^{\triangle ij_1k_1}(\alpha^*,v(t)) \\ &+ \sum_{(j_2,i,k_2)\in\bar{\mathcal{A}}} (A_i^{\triangle j_2ik_2}(\alpha^*))^\top f_i^{\triangle j_2ik_2}(\alpha^*,v(t)) \\ &+ \sum_{(j_3,k_3,i)\in\bar{\mathcal{A}}} (A_i^{\triangle j_3k_3i}(\alpha^*))^\top f_i^{\triangle j_3k_3i}(\alpha^*,v(t))\Bigg] \end{aligned} \tag{16}$$

where $f_i^{\triangle ij_1k_1}(\alpha^*,p(t)) = \sin\alpha^*_{j_1k_1i}(p_i(t) - p_{k_1}(t)) - \sin\alpha^*_{ij_1k_1} R^\top(\alpha^*_{k_1ij_1})(p_i(t) - p_{j_1}(t))$ is the weighted sum of the relative position measurements $(p_i - p_{k_1})$ and $(p_i - p_{j_1})$, $\{k_1, j_1\} \in \mathcal{N}_i$, and similarly $f_i^{\triangle j_2ik_2}(\alpha^*,p(t)) = \sin\alpha^*_{ik_2j_2}(p_{j_2}(t) - p_{k_2}(t)) - \sin\alpha^*_{j_2ik_2}R^\top(\alpha^*_{k_2j_2i})(p_{j_2}(t) - p_i(t))$, and $\bar{\mathcal{A}}$ is a subset of $\mathcal{A}$ satisfying $|\bar{\mathcal{A}}| = n^\triangle_{\mathcal{A}}$ such that $(i,j,k) \in \bar{\mathcal{A}}$ then $(j,k,i) \notin \bar{\mathcal{A}}, (k,i,j) \notin \bar{\mathcal{A}}$. Note that $p_{j_2}(t) - p_{k_2}(t)$ can be obtained by the measurements of $p_{j_2}(t) - p_i(t)$ and $p_i(t) - p_{k_2}(t)$. It can be seen that the maneuvering control law (16) only requires each follower $i \in \mathcal{V}_f$ to have relative position $p_i - p_j$ and relative velocity $v_i - v_j$ measurements with respect to its neighbors $j \in \mathcal{N}_i$. Now, we present the main results.

Theorem 1: If the desired triangular angularity $\mathbb{A}^*(\mathcal{V},\mathcal{A},p^*)$ is angle rigid and the two leaders have constant velocities, then under control law (16), the formation maneuvering objective (6) is achieved with a global convergence guarantee.

Proof: The designed control law (16) is linear with respect to the agents' positions p, which is always well-defined even when an inter-agent collision occurs. Substituting the control law (15) into (5), one has

$$\ddot{\tilde{p}}_f(t) + k_v\mathcal{L}_{ff}(\alpha^*)\dot{\tilde{p}}_f(t) + k_p\mathcal{L}_{ff}(\alpha^*)\tilde{p}^f(t) = 0 \tag{17}$$

where we have used the fact that the two leaders have constant maneuvering velocities, i.e., $\ddot{p}^l(t) = 0$. Since the coefficient matrix $\mathcal{L}_{ff}(\alpha^*)$ in (17) is constant, the characteristic polynomial of the dynamical system (17) can be written as

$$\det[\lambda^2 I_{2N-4} + k_v\mathcal{L}_{ff}(\alpha^*)\lambda + k_p\mathcal{L}_{ff}(\alpha^*)] = 0 \tag{18}$$

where $\lambda \in \mathbb{C}$ represents the solution of (18). Since $\mathcal{L}_{ff}(\alpha^*)$ is positive definite, there must exist a nonsingular real matrix $Q \in \mathbb{R}^{(2N-4)\times(2N-4)}$ such that $\mathcal{L}_{ff}(\alpha^*) = Q\mathrm{diag}[a_1,\ldots, a_{2N-4}]Q^{-1}$, where $a_i > 0$ represents the ith real eigenvalue of $\mathcal{L}_{ff}(\alpha^*)$. Then, one has

$$\det[\lambda^2 I_{2N-4} + k_v\mathcal{L}_{ff}(\alpha^*)\lambda + k_p\mathcal{L}_{ff}] = \prod_{i=1}^{2N-4}(\lambda^2 + k_va_i\lambda + k_pa_i).$$

Since $k_p > 0, k_v > 0$, all the solutions associated with the polynomial (18) have negative real parts. Therefore, $\tilde{p}(t)$ and $\tilde{v}_f(t) = \dot{\tilde{p}}_f(t)$ will globally and exponentially converge to zero. ■

Now, we provide a toy example to illustrate the controller (16).

Example 1: Consider that agents 1 and 2 are the leaders, agent 3 is the follower, and $\bar{\mathcal{A}} = \{(1,2,3)\}$. Following the definitions given after (16), the control law for agent 3 can be written by:

$$\begin{aligned} u_3 = &-k_pA_3^{\triangle 123}(\alpha^*)(\sin\alpha^*_{231}(p_1 - p_3) - \sin\alpha^*_{123}R^\top(\alpha^*_{312}) \\ &\times(p_1 - p_2)) - k_vA_3^{\triangle 123}(\alpha^*)\Big(\sin\alpha^*_{231}(v_1 - v_3) \\ &- \sin\alpha^*_{123}R^\top(\alpha^*_{312})(v_1 - v_2)\Big) \end{aligned}$$

where $p_1 - p_2 = (p_1 - p_3) - (p_2 - p_3)$ can be obtained from the measurements of $p_1 - p_3$ and $p_2 - p_3$, and $A_3^{\triangle 123}(\alpha^*)$ follows the definition given in (10).

Remark 1: Compared with the previous results [7], [25], [27] on maneuvering angle rigid formations with local or almost global convergence guarantees, the designed maneuvering law (15) can guarantee global convergence. This is mainly because of the transformation of the nonlinear angle constraints (3) imposed on each triangle into linear algebraic equations (11). In addition, although this paper only considers double-integrator dynamics for the followers, formation maneuvering laws for single-integrator dynamics can be similarly obtained by following [5].

Remark 2: Suppose that each follower $i \in \mathcal{V}_f$ holds a local coordinate frame $\sum_i$ to measure the relative positions and velocities with respect to its neighbors. Taking the first component $(A_i^{\triangle ij_1k_1}(\alpha^*))^\top f_i^{\triangle ij_1k_1}(\alpha^*, p(t))$ in (16) as an example, one has that $f_i^{\triangle ij_1k_1}(\alpha^*, p(t))$ measured in agent i's local coordinate frame $\sum_i$ becomes $\sin\alpha^*_{j_1k_1i} R_g^i \left(p_i(t) - p_{k_1}(t)\right) = R_g^i f_i^{\triangle ij_1k_1}(\alpha^*, p(t))$. It follows that the first component measured in $\sum_i$ becomes $R_g^i (A_i^{\triangle ij_1k_1}(\alpha^*))^\top f_i^{\triangle ij_1k_1}(\alpha^*, p(t))$. For the remaining components in (16), one can obtain similar forms. By following [23], it can be verified that the control law (16) can be implemented in each agent's local coordinate frame. This is an advantage compared with those displacement-constrained or bearing rigid formations that requires all agents to have aligned coordinate frames.

C. Maneuvering Control for the Case Of Leaders With Time-Varying Velocities

Since the angle constraints in $f_{\mathcal{A}}(\alpha^*)$ are invariant to the formation's translation, rotation and scaling, the full maneuvering of translation, rotation and scaling can be achieved by commanding the two leaders to move with the correspondingly translational, rotational and scaling velocities, respectively. Specifically, one can manipulate the parameters in the two leaders' moving trajectories (4) to achieve:

1) Translational Maneuvering: $\dot{s}(t) = 0, \dot{\theta}(t) = 0, \dot{w}(t) \neq 0$;

2) Rotational Maneuvering: $\dot{s}(t) = 0, \theta(t) = \omega_c t, \dot{w}(t) = 0$, where ω_c is a constant scalar;

3) Scaling Maneuvering: $\dot{s}(t) \neq 0, \dot{\theta}(t) = 0, \dot{w}(t) = 0$.

However, if the desired maneuvering includes a rotational maneuvering, then $\ddot{p}^l(t) \neq 0$, which cannot be handled by (16). Therefore, we now discuss the extension of the maneuvering algorithm (16) into the case in which the two leaders have time-varying velocities, i.e., $\ddot{p}^l(t) \neq 0$.

When $\ddot{p}^l(t)$ can be measured by some followers (or measured by the leaders and communicated to some followers), one can employ consensus-based distributed estimators to design the formation maneuvering law, see e.g., [5], [13], [29], [33]. Instead, we discuss the case where the leaders' accelerations are unavailable, and employ the sliding model control approach to design the maneuvering control law. According to [34, Section II.B.2], a sliding mode-based reaching law can be designed as $\dot{s}(x) = -\gamma_1 \text{sign}(s(x)) - k_1 s(x)$ where γ_1 and k_1 are positive scalars, and $s(x)$ is the sliding surface. Based on the above sliding mode-based reaching law, we design the sliding surface as

$$s^f(t) = k_v\left[\mathcal{L}_{ff}(\alpha^*)v^f(t) + \mathcal{L}_{fl}(\alpha^*)v^l(t)\right] + k_p\mathcal{L}_{ff}(\alpha^*)\left[\mathcal{L}_{ff}(\alpha^*)p^f(t) + \mathcal{L}_{fl}(\alpha^*)p^l(t)\right] \quad (19)$$

where $s^f = [s_3^\top, \ldots, s_N^\top]^\top \in \mathbb{R}^{2N-4}$. Inspired by [29], we design the sliding mode-based maneuvering law as

$$u^f = -\gamma_1 \text{sign}(s^f) - k_1 s^f - \frac{k_p}{k_v}[\mathcal{L}_{ff}(\alpha^*)v^f + \mathcal{L}_{fl}(\alpha^*)v^l] \quad (20)$$

where k_1 is a positive scalar.

Theorem 2: If the desired triangular angularity $\mathbb{A}^*(\mathcal{V}, \mathcal{A}, p^*)$ is angle rigid, the two leaders have bounded time-varying velocities, and γ_1 is sufficiently large, then under (20), the formation maneuvering objective (6) is achieved with a global convergence guarantee.

Proof: Taking the time-derivative of (19) and using (20) yield

$$\begin{aligned}\dot{s}^f &= k_v\left[\mathcal{L}_{ff}(\alpha^*)\ddot{p}^f(t) + \mathcal{L}_{fl}(\alpha^*)\ddot{p}^l(t)\right] \\ &\quad + k_p\mathcal{L}_{ff}(\alpha^*)\left[\mathcal{L}_{ff}(\alpha^*)v^f(t) + \mathcal{L}_{fl}(\alpha^*)v^l(t)\right] \\ &= k_v\left[\mathcal{L}_{ff}(\alpha^*)(-\gamma_1 \text{sign}(s^f) - k_1 s^f) + \mathcal{L}_{fl}(\alpha^*)\ddot{p}^l(t)\right].\end{aligned}$$

Now, we prove the stability by constructing the Lyapunov function as $V_2 = 0.5(s^f)^\top \mathcal{L}_{ff}^{-1}(\alpha^*)s^f > 0$. Taking the time-derivative of V_2 yields

$$\begin{aligned}\dot{V}_2 &= k_v(s^f)^\top\left[-\gamma_1 \text{sign}(s^f) - k_1 s^f + \mathcal{L}_{ff}^{-1}(\alpha^*)\mathcal{L}_{fl}(\alpha^*)\ddot{p}^l(t)\right] \\ &= -k_v\gamma_1\|s^f\|_1 - k_1 k_v s^{f\top}s^f + k_v s^{f\top}\mathcal{L}_{ff}^{-1}(\alpha^*)\mathcal{L}_{fl}(\alpha^*)\ddot{p}^l(t).\end{aligned} \quad (21)$$

Using the facts $(s^f)^\top\mathcal{L}_{ff}^{-1}(\alpha^*)\mathcal{L}_{fl}(\alpha^*)\ddot{p}^l(t) \leq \|s^f\|_2\|\mathcal{L}_{ff}^{-1}(\alpha^*) \times \mathcal{L}_{fl}(\alpha^*)\|_2\|\ddot{p}^l(t)\|_2$ and $\|s^f\|_1 \geq \|s^f\|_2$ yields

$$\begin{aligned}\dot{V}_2 \leq &-k_1 k_v\|s^f\|^2 \\ &- k_v\left(\gamma_1 - \|\mathcal{L}_{ff}^{-1}(\alpha^*)\mathcal{L}_{fl}(\alpha^*)\|_2\|\ddot{p}^l(t)\|_2\right)\|s^f\|_2.\end{aligned} \quad (22)$$

Since $\|\mathcal{L}_{ff}^{-1}(\alpha^*)\mathcal{L}_{fl}(\alpha^*)\|_2$ is constant and $\|\ddot{p}^l(t)\|_2$ is upper bounded, one can choose sufficiently large γ_1 such that $\gamma_1 > \gamma_2 := \sup_{t\geq 0}\|\mathcal{L}_{ff}^{-1}(\alpha^*)\mathcal{L}_{fl}(\alpha^*)\|_2\|\ddot{p}^l(t)\|_2$, under which $\dot{V}_2 \leq -2k_1k_v\lambda_{\min}(\mathcal{L}_{ff})V_2 - k_v(\gamma_1 - \gamma_2)\sqrt{2\lambda_{\min}(\mathcal{L}_{ff})}V_2^{\frac{1}{2}}$. It follows from [34] that s^f converges to zero within a finite time. Since $\mathcal{L}_{ff}(\alpha^*) > 0$ in (19), using the input-to-state stability theorem for (19), one has $\left(\mathcal{L}_{ff}(\alpha^*)p^f(t) + \mathcal{L}_{fl}(\alpha^*)p^l(t)\right) \to 0$, i.e., the desired formation maneuvering is achieved with a global convergence guarantee. ■

At the formation design stage, one can use the information of $\mathcal{L}_{ff}(\alpha^*), \mathcal{L}_{fl}(\alpha^*)$, and $\|\ddot{p}^l(t)\|_2$ to properly select γ_1. Due to the second component of s^f in (19), the sliding mode-based maneuvering law (20) indeed needs the communication among the neighboring followers. However, the acceleration estimation and the leaders' acceleration measurements are not needed in (20) [29].

IV. Maneuvering 3D Angle Rigid Formations

To globally maneuver 3D angle rigid formations by employing angle-induced linear equations, it has been demonstrated in [8] that the construction of each angle-induced linear equation needs to associate at least five agents. This indicates that each agent should have relative position measurements with respect to at least four neighbors. To reduce the number of neighbors that each agent should have, we propose to associate only four agents to construct an angle-induced linear equation under the following assumption.

Assumption 1: Assume in 3D that all the agents' coordinate frames have a common Z direction.

Different from [35], [36] where an additional virtual coordinate is assigned to each agent, Assumption 1 practically requires the agents to have the sensing capability of the direction of the global Z-axis, which can be fulfilled by equipping each agent with a gravity sensor or extracting a common vertical direction via image processing [37]. In the follow-up subsections, we first introduce an angle-induced linear equation established on a tetrahedron, then define the desired Z-weakly angle rigid formation, and finally design the formation maneuvering law for the followers.

A. Angle-Induced Linear Equations in Tetrahedra

A shown in Fig. 1, we take four agents 1, 2, 3, 4 in a tetrahedron as an example to illustrate the process of establishing an angle-induced linear equation among them. Consider a coordinate frame $\sum_{1-XYZ}$ whose origin is p_1 and X,Y,Z-axes point towards the same directions as the X,Y,Z-axes of $\sum_g$, respectively. For a non-coplanar tetrahedron $\lozenge 1234$, we perpendicularly project the three points 2, 3, and 4 into the $X1Y$ plane, and then get the projected points $2'$, $3'$, and $4'$, respectively.

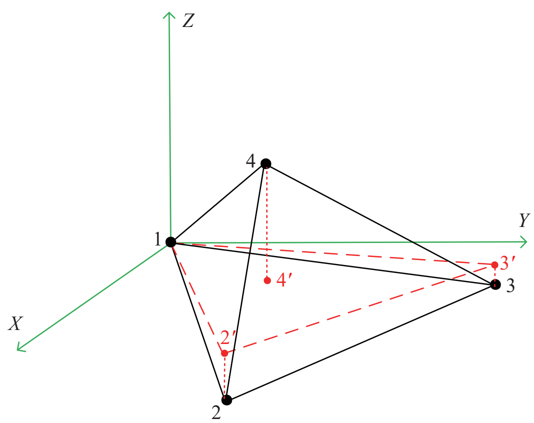

Fig. 1. Establish an angle-induced linear equation for $\lozenge 1234$.

According to the planar angle-induced linear equations (8) existing in 2D triangles, two angle-induced linear equations existing in the planar $\triangle 2'14'$ and $\triangle 4'13'$ can be written as

$$(p_{2'}-p_1)/\|p_{2'}-p_1\| = R_z(\alpha_{4'12'})(p_{4'}-p_1)/\|p_{4'}-p_1\| \quad (23)$$

$$(p_{3'}-p_1)/\|p_{3'}-p_1\| = R_z(\alpha_{4'13'})(p_{4'}-p_1)/\|p_{4'}-p_1\| \quad (24)$$

where $R_z(\alpha_{4'12'}) = \begin{bmatrix} R(\alpha_{4'12'}) & 0 \\ 0 & 1 \end{bmatrix} \in SO(3)$ is the rotation matrix along the Z-axis, $\alpha_{4'12'} \in [0,2\pi), \alpha_{4'13'} \in [0,2\pi)$ are signed angles whose definition follows (7), and $p_{i'} \in \mathbb{R}^3, i=2,3,4$ are the positions of i' in $\sum_g$. We consider in this section that except for $\alpha_{4'12'}, \alpha_{4'13'}$ or generally $\alpha_{m_1' i_1 j_1'}, \alpha_{m_1' i_1 k_1'}, \mathcal{S}_{\lozenge i_1 j_1 k_1 m_1} \in \mathcal{A}$, all the other angles' magnitude is within $[0,\pi]$. Assume that $1,2',4'$ are not collinear, and that $1,4',3'$ are not collinear. According to the law of sines, $p_{i'}, i=2,3,4$ satisfy

$$\frac{\|p_{2'}-p_1\|}{\|p_{4'}-p_1\|} = \frac{\sin\alpha_{2'4'1}}{\sin\alpha_{4'2'1}}, \quad \frac{\|p_{3'}-p_1\|}{\|p_{4'}-p_1\|} = \frac{\sin\alpha_{3'4'1}}{\sin\alpha_{4'3'1}}. \quad (25)$$

Since the vectors $p_{i'}-p_1$ are a projection of p_i-p_1 to the X1Y plane, the relation between p_i and $p_{i'}$ can be described by

$$p_{i'}-p_1 = \begin{bmatrix} 1 & 0 & 0 \\ 0 & 1 & 0 \\ 0 & 0 & 0 \end{bmatrix}(p_i-p_1), i=2,3,4. \quad (26)$$

Substituting (25) and (26) into (23) yields

$$\sin\alpha_{4'2'1}(p_{2xy}-p_{1xy}) = \sin\alpha_{2'4'1}R(\alpha_{4'12'})(p_{4xy}-p_{1xy}) \quad (27)$$

where $p_{ixy} = [p_i(1), p_i(2)]^\top \in \mathbb{R}^2, i=1,2,3,4$, $p_i(j)$ represents the jth element of the vector p_i. Similarly, substituting (25) and (26) into (24) yields

$$\sin\alpha_{4'3'1}(p_{3xy}-p_{1xy}) = \sin\alpha_{3'4'1}R(\alpha_{4'13'})(p_{4xy}-p_{1xy}). \quad (28)$$

Note that (27) and (28) represent the final angle-induced linear equations of the nodes 1, 2, 3, and 4 in the $X1Y$ plane, which is valid under the assumption that $1,2',4'$ are not collinear, and $1,4',3'$ are not collinear. However, if $1,2',4'$ are collinear, then (27) will be degraded into a trivial equation.

Instead of focusing on the $X1Y$ plane, we now establish Z directional constraints among the four points. Suppose that p_2, p_3, p_4 are not in the $X1Y$ plane. According to Fig. 1, the Z directional constraints can be described as

$$\begin{aligned} \operatorname{sgn}(\sin\alpha_{21Z})\frac{p_{2z}-p_{1z}}{\|p_{2z}-p_{1z}\|} &= \operatorname{sgn}(\sin\alpha_{31Z})\frac{p_{3z}-p_{1z}}{\|p_{3z}-p_{1z}\|} \\ \operatorname{sgn}(\sin\alpha_{21Z})\frac{p_{2z}-p_{1z}}{\|p_{2z}-p_{1z}\|} &= \operatorname{sgn}(\sin\alpha_{41Z})\frac{p_{4z}-p_{1z}}{\|p_{4z}-p_{1z}\|} \end{aligned} \quad (29)$$

where $p_{iz} = p_i(3), i=1,2,3,4$, and the sgn() function is used to distinguish the different sign of $(p_i)'s$ Z coordinates with respect to the $X1Y$ plane. For (29), using the law of sines in $\triangle 212'$, $\triangle 313'$ and $\triangle 213$, one has $\frac{\operatorname{sgn}(\sin\alpha_{31Z})\|p_{2z}-p_{1z}\|}{\operatorname{sgn}(\sin\alpha_{21Z})\|p_{3z}-p_{1z}\|} = \frac{\cos\alpha_{21Z}\sin\alpha_{231}}{\cos\alpha_{31Z}\sin\alpha_{321}}$, where $\alpha_{212'}, \alpha_{313'}, \alpha_{231}, \alpha_{321}$ are scalar angles, and we have used the facts that $\cos\alpha_{21Z} = \sin\alpha_{212'} \times \operatorname{sgn}(\sin\alpha_{21Z})$ and $\frac{\operatorname{sgn}(\sin\alpha_{31Z})}{\operatorname{sgn}(\sin\alpha_{21Z})} = \frac{\operatorname{sgn}(\sin\alpha_{21Z})}{\operatorname{sgn}(\sin\alpha_{31Z})}$. Similarly, one also has $\frac{\operatorname{sgn}(\sin\alpha_{41Z})\|p_{2z}-p_{1z}\|}{\operatorname{sgn}(\sin\alpha_{21Z})\|p_{4z}-p_{1z}\|} = \frac{\cos\alpha_{21Z}\sin\alpha_{241}}{\cos\alpha_{41Z}\sin\alpha_{421}}$. Then, it follows that:

$$\begin{aligned} \cos\alpha_{31Z}\sin\alpha_{321}(p_{2z}-p_{1z}) &= \cos\alpha_{21Z}\sin\alpha_{231}(p_{3z}-p_{1z}) \\ \cos\alpha_{41Z}\sin\alpha_{421}(p_{2z}-p_{1z}) &= \cos\alpha_{21Z}\sin\alpha_{241}(p_{4z}-p_{1z}) \end{aligned} \quad (30)$$

which are the two remaining angle-induced linear constraints of $\lozenge 1234$. However, if p_2, p_3, p_4 are in the $X1Y$ plane, then (30) will be reduced to trivial equations.

By summarizing (27)–(30), the overall angle-induced linear equations among agents 1, 2, 3, 4 can be described by

$$\begin{aligned} f_1^{\lozenge 1234}(\alpha,p) = {} & A_1^{\lozenge 1234}(\alpha)p_1 + A_2^{\lozenge 1234}(\alpha)p_2 \\ & + A_3^{\lozenge 1234}(\alpha)p_3 + A_4^{\lozenge 1234}(\alpha)p_4 = 0 \end{aligned} \quad (31)$$

where $A_i^{\lozenge 1234} \in \mathbb{R}^{6\times 3}, i=1,\ldots,4$ are defined as $A_1^{\lozenge 1234} = \begin{bmatrix} \sin\alpha_{2'4'1}R(\alpha_{4'12'}) - \sin\alpha_{4'2'1}I_2 & 0_{2\times 1} \\ 0_{1\times 2} & a_{11} - a_{12} \\ \sin\alpha_{3'4'1}R(\alpha_{4'13'}) - \sin\alpha_{4'3'1}I_2 & 0_{2\times 1} \\ 0_{1\times 2} & a_{21} - a_{22} \end{bmatrix}$, $A_2^{\lozenge 1234} = \begin{bmatrix} \sin\alpha_{4'2'1}I_2 & 0_{2\times 1} \\ 0_{1\times 2} & a_{12} \\ 0_{2\times 2} & 0_{2\times 1} \\ 0_{1\times 2} & a_{22} \end{bmatrix}$, $A_3^{\lozenge 1234} = \begin{bmatrix} 0_{2\times 2} & 0_{2\times 1} \\ 0_{1\times 2} & -a_{11} \\ \sin\alpha_{4'3'1}I_2 & 0_{2\times 1} \\ 0_{1\times 2} & 0_{1\times 1} \end{bmatrix}$, $A_4^{\lozenge 1234} = \begin{bmatrix} -\sin\alpha_{2'4'1}R(\alpha_{4'12'}) & 0_{2\times 1} \\ 0_{1\times 2} & 0_{1\times 1} \\ -\sin\alpha_{3'4'1}R(\alpha_{4'13'}) & 0_{2\times 1} \\ 0_{1\times 2} & -a_{21} \end{bmatrix}$, $a_{11} = \cos\alpha_{21Z}\sin\alpha_{231}$, $a_{12} = \cos\alpha_{31Z}\sin\alpha_{321}$, $a_{21} = \cos\alpha_{21Z}\sin\alpha_{241}$, $a_{22} = \cos\alpha_{41Z}\sin\alpha_{421}$. It is obvious that $A_1^{\lozenge 1234}(\alpha) + A_2^{\lozenge 1234}(\alpha) + A_3^{\lozenge 1234}(\alpha) +$

$A_4^{\triangle 1234}(\alpha)=0$. Note that the coefficient matrices $A_i^{\triangle 1234}\in\mathbb{R}^{6\times 3}, i=1,\ldots,4$ are only related with the interior angles of $\triangle 1234$ and the angles formed by the edges of $\triangle 1234$ and the Z-axis. Moreover, according to the definition of the angles shown in $A_i^{\triangle 1234}\in\mathbb{R}^{6\times 3}, i=1,\ldots,4$, one has that $A_i^{\triangle 1234}, i=1,\ldots,4$ are invariant with respect to $\triangle 1234$'s translation, scaling, and rotation along the Z-axis.

Lemma 2: For a tetrahedron $\triangle 1234$ with projected points $2', 3', 4'$, if $1, 2', 4'$ are not collinear, and $1, 4', 3'$ are not collinear, and p_2, p_3, p_4 are not in the $X1Y$ plane, then

$$\mathrm{Rank}[A_1^{\triangle 1234}(\alpha), A_2^{\triangle 1234}(\alpha), A_3^{\triangle 1234}(\alpha), A_4^{\triangle 1234}(\alpha)]=6.$$

Proof: Construct a submatrix $S_1\in\mathbb{R}^{6\times 6}$ from the matrix $[A_1^{\triangle 1234}(\alpha), A_2^{\triangle 1234}(\alpha), A_3^{\triangle 1234}(\alpha), A_4^{\triangle 1234}(\alpha)]$ as

$$S_1=\begin{bmatrix}\sin\alpha_{4'2'1}I_2 & 0_{2\times 2} & 0_{2\times 1} & 0_{2\times 1}\\ 0_{1\times 2} & 0_{1\times 2} & -a_{11} & 0_{1\times 1}\\ 0_{2\times 2} & \sin\alpha_{4'3'1}I_2 & 0_{2\times 1} & 0_{2\times 1}\\ 0_{1\times 2} & 0_{1\times 2} & 0_{1\times 1} & -a_{21}\end{bmatrix}. \tag{32}$$

One can easily verify that under the given assumptions, $6\geq\mathrm{Rank}(S)\geq\mathrm{Rank}(S_1)=6$, which completes the proof. ■

The above analysis takes $\triangle 1234$ as an example. Now, we consider a tetrahedral angularity $\mathbb{A}(\mathcal{V},\mathcal{A},p)$ with multiple tetrahedra defined in the tetrahedral angle set $\mathcal{A}$. One can write all the angle-induced linear equations from the tetrahedral angularity $\mathbb{A}(\mathcal{V},\mathcal{A},p)$ into a compact form

$$\bar{M}_{\mathcal{A}}(\alpha(p))p=0 \tag{33}$$

where $\bar{M}_{\mathcal{A}}(\alpha(p))\in\mathbb{R}^{6n_{\mathcal{A}}^{\triangle}\times 3N}$ can be written by

$$\begin{array}{c} \\ \text{1st}\,\triangle \\ \cdots \\ \triangle ijkm \\ \cdots \\ n_A^{\triangle}\text{th}\,\triangle \end{array}
\begin{array}{c} \cdots\ \text{Vertex } i\ \cdots\ \text{Vertex } j\ \cdots\ \text{Vertex } k\ \cdots\ \text{Vertex } m\ \cdots \\
\begin{bmatrix} \cdots & \cdots & \cdots & \cdots & \cdots & \cdots & \cdots & \cdots & \cdots\\ \cdots & \cdots & \cdots & \cdots & \cdots & \cdots & \cdots & \cdots & \cdots\\ 0 & A_i^{\triangle ijkm} & 0 & A_j^{\triangle ijkm} & 10 & A_k^{\triangle ijkm} & 0 & A_m^{\triangle ijkm} & 0\\ \cdots & \cdots & \cdots & \cdots & \cdots & \cdots & \cdots & \cdots & \cdots\\ \cdots & \cdots & \cdots & \cdots & \cdots & \cdots & \cdots & \cdots & \cdots \end{bmatrix}\end{array} \tag{34}$$

whose row blocks are indexed by the tetrahedra defined in the tetrahedral angle set $\mathcal{A}$ and column blocks are indexed by the vertices.

B. Desired Z-Weakly Angle Rigid Formations and Their Properties

Note that the angle-induced linear equation (31) is associated with not only the interior angles in $\triangle 1234$, but also the angles formed by the edges of $\triangle 1234$ and the Z-axis. Therefore, except for the angles defined in the tetrahedral angle set $\mathcal{A}$, we need to additionally impose angle constraints formed by the edges of $\triangle 1234$ and the Z-axis such that these coefficient matrices in (31) can be uniquely determined. Towards this end, we first define a set mapping such that these additional angle constraints can be included in a new angle set.

Definition 2: For a tetrahedral angle set[2] $\mathcal{A}=\{\mathcal{S}_{\triangle i_1j_1k_1m_1},\ldots,\mathcal{S}_{\triangle i_{n_{\mathcal{A}}^{\triangle}}j_{n_{\mathcal{A}}^{\triangle}}k_{n_{\mathcal{A}}^{\triangle}}m_{n_{\mathcal{A}}^{\triangle}}}\}$, define the set mapping $\mathcal{M}$ as

$$\mathcal{M}:\mathcal{A}\to\bar{\mathcal{A}}:=\{\mathcal{S}_{\triangle i_1j_1k_1m_1},(j_1,i_1,Z),(k_1,i_1,Z),(m_1,i_1,Z),\ldots,\mathcal{S}_{\triangle i_{n_{\mathcal{A}}^{\triangle}}j_{n_{\mathcal{A}}^{\triangle}}k_{n_{\mathcal{A}}^{\triangle}}m_{n_{\mathcal{A}}^{\triangle}}},(j_{n_{\mathcal{A}}^{\triangle}},i_{n_{\mathcal{A}}^{\triangle}},Z),(k_{n_{\mathcal{A}}^{\triangle}},i_{n_{\mathcal{A}}^{\triangle}},Z),(m_{n_{\mathcal{A}}^{\triangle}},i_{n_{\mathcal{A}}^{\triangle}},Z)\}$$

where (j_1,i_1,Z) describes the angle constraint formed by the rays $\overrightarrow{i_1j_1}$ and $\overrightarrow{i_1Z}$.

Definition 3: A 3D angularity $\bar{\mathbb{A}}(\mathcal{V},\bar{\mathcal{A}},p)$ where p is generic, $\bar{\mathcal{A}}$ is obtained from $\mathcal{A}$ under the mapping $\mathcal{M}$, and $\mathcal{A}$ is a tetrahedral angle set, is said to be Z-weakly angle rigid if

$$\begin{aligned}&\{p'|\alpha_{jik}(p')=\alpha_{jik}(p),\forall(j,i,k)\in\bar{\mathcal{A}}\}\\ &\quad=\{p'|p'=s_c[I_N\otimes R_z(\theta_c)]p+1_N\otimes w_c, s_c\in\mathbb{R}^+,\\ &\quad\quad\theta_c\in\mathbb{R}, w_c\in\mathbb{R}^3\}\end{aligned}$$

i.e., to maintain the given angle constraints in $\bar{\mathcal{A}}$, $\bar{\mathbb{A}}$ can only translate, scaling, and rotate along the Z-axis.

Before presenting the results, we first need to make an assumption.

Assumption 2: For each tetrahedron $\triangle ijkm$ in the desired 3D tetrahedral angularity $\mathbb{A}(\mathcal{V},\mathcal{A},p^*)$ with generic p^*, we assume that i, j', m' are not collinear, i, k', m' are not collinear, and p_j^*, p_k^*, p_m^* are not in i's XiY plane.

Now, we have the following theorem.

Theorem 3: For a 3D Z-weakly angle rigid angularity $\bar{\mathbb{A}}(\mathcal{V},\bar{\mathcal{A}},p)$, if Assumption 2 holds, then $\mathrm{Rank}(\bar{M}_{\mathcal{A}}(\alpha(p)))=3N-6$ and $\mathrm{Span}\{p,(I_N\otimes R_z(\varphi))p, 1_N\otimes[1,0,0]^\top, 1_N\otimes[0,1,0]^\top, 1_N\otimes[0,0,1]^\top\}\subseteq\mathrm{Null}(\bar{M}_{\mathcal{A}}(\alpha(p)))$, where $\varphi\in\mathbb{R}$ is an arbitrary number.

Proof: We first prove the null space of $\bar{M}_{\mathcal{A}}(\alpha(p))$. Since $A_i^{\triangle ijkm}(\alpha)+A_j^{\triangle ijkm}(\alpha)+A_k^{\triangle ijkm}(\alpha)+A_m^{\triangle ijkm}(\alpha)=0$, $\{1_N\otimes[1,0,0]^\top, 1_N\otimes[0,1,0]^\top, 1_N\otimes[0,0,1]^\top\}$ lie in the null space of $\bar{M}_{\mathcal{A}}(\alpha(p))$. Then, according to (31) one has

$$\begin{aligned}f_i^{\triangle ijkm}(\alpha,p)&=A_i^{\triangle ijkm}(\alpha)p_i+A_j^{\triangle ijkm}(\alpha)p_j+A_k^{\triangle ijkm}(\alpha)p_k\\ &\quad+A_m^{\triangle ijkm}(\alpha)p_m=0\end{aligned} \tag{35}$$

which implies that p lies in the null space of $\bar{M}_{\mathcal{A}}(\alpha(p))$. To prove that $(I_N\otimes R_z(\varphi))p$ also lies in the null space of $\bar{M}_{\mathcal{A}}(\alpha(p))$, we need to check

$$\begin{aligned}f_i^{\triangle ijkm}(\alpha,(I_N\otimes R_z(\varphi))p)&=A_i^{\triangle ijkm}(\alpha)R_z(\varphi)p_i\\ &\quad+A_j^{\triangle ijkm}(\alpha)R_z(\varphi)p_j+A_k^{\triangle ijkm}(\alpha)R_z(\varphi)p_k\\ &\quad+A_m^{\triangle ijkm}(\alpha)R_z(\varphi)p_m.\end{aligned} \tag{36}$$

Taking $A_m^{\triangle ijkm}(\alpha)R_z(\varphi)$ in (36) as an example, one has

$$\begin{aligned}&A_m^{\triangle ijkm}(\alpha)R_z(\varphi)\\ &=\begin{bmatrix}\begin{bmatrix}-\sin\alpha_{j'm'i}R(\alpha_{m'ij'}) & 0_{2\times 1}\\ 0_{1\times 2} & 0_{1\times 1}\end{bmatrix}R_z(\varphi)\\ \begin{bmatrix}-\sin\alpha_{k'm'i}R(\alpha_{m'ik'}) & 0_{2\times 1}\\ 0_{1\times 2} & -\cos\alpha_{jiZ}\sin\alpha_{jmi}\end{bmatrix}R_z(\varphi)\end{bmatrix}\\ &=\begin{bmatrix}R_z(\varphi)\begin{bmatrix}-\sin\alpha_{j'm'i}R(\alpha_{m'ij'}) & 0_{2\times 1}\\ 0_{1\times 2} & 0_{1\times 1}\end{bmatrix}\\ R_z(\varphi)\begin{bmatrix}-\sin\alpha_{k'm'i}R(\alpha_{m'ik'}) & 0_{2\times 1}\\ 0_{1\times 2} & -\cos\alpha_{jiZ}\sin\alpha_{jmi}\end{bmatrix}\end{bmatrix}\\ &=\begin{bmatrix}R_z(\varphi) & 0\\ 0 & R_z(\varphi)\end{bmatrix}A_m^{\triangle ijkm}(\alpha)=[I_2\otimes R_z(\varphi)]A_m^{\triangle ijkm}(\alpha)\end{aligned} \tag{37}$$

[2] Although $\mathcal{S}_{\triangle i_1j_1k_1m_1}\cap\mathcal{S}_{\triangle i_2j_2k_2m_2}$ may be nonempty, this will not affect the total effective number of angle constraints in $\mathcal{A}$.

where we used $R_z(\varphi)=\begin{bmatrix}R(\varphi) & 0_{2\times1}\\ 0_{1\times2} & 1\end{bmatrix}$ and $R(\alpha_{m'ij'})R(\varphi)=R(\varphi)R(\alpha_{m'ij'})$. Substituting (37) into (36) yields

$$f_i^{\triangle ijkm}(\alpha,(I_N\otimes R_z(\varphi))p)=[I_2\otimes R_z(\varphi)]f_i^{\triangle ijkm}(\alpha,p)=0$$

i.e., $(I_N\otimes R_z(\varphi))p$ lies in the null space of $\bar{M}_{\mathcal{A}}(\alpha(p))$.

Finally, we prove that $\text{Rank}(\bar{M}_{\mathcal{A}}(\alpha(p)))=3N-6$. According to the Euler-Rodrigues formula, $R_z(\varphi)$ can be written as

$$R_z(\varphi)=\cos\varphi I_3+\sin\varphi B_1+(1-\cos\varphi)B_2 \qquad (38)$$

where $B_1=\begin{bmatrix}0 & -1 & 0\\ 1 & 0 & 0\\ 0 & 0 & 0\end{bmatrix}, B_2=\begin{bmatrix}0 & 0 & 0\\ 0 & 0 & 0\\ 0 & 0 & 1\end{bmatrix}$. Therefore, the vector $(I_N\otimes R_z(\varphi))p$ can be decomposed into three components, where the first component $(\cos\varphi)p$ is linearly dependent of p, and the remaining two components $\sin\varphi(I_N\otimes B_1)p,(1-\cos\varphi)(I_N\otimes B_2)p$ are linearly independent of $\{p,1_N\otimes[1,0,0]^\top, 1_N\otimes[0,1,0]^\top,1_N\otimes[0,0,1]^\top\}$. Therefore, there are at least six linearly independent vectors lying in the null space of $\bar{M}_{\mathcal{A}}(\alpha(p))$, i.e., $\text{Rank}(\bar{M}_{\mathcal{A}}(\alpha(p)))\le 3N-6$. Now, suppose that $\text{Rank}(\bar{M}_{\mathcal{A}}(\alpha(p)))<3N-6$, i.e., there exists at least one nonzero vector $\bar{v}\in\mathbb{R}^{3N}$ such that $\bar{M}_{\mathcal{A}}(\alpha(p))\bar{v}=0$ and $\bar{v}$ is linearly independent of the aforementioned six vectors in the kernel of $\bar{M}_{\mathcal{A}}(\alpha(p))$. According to the structure of $\bar{M}_{\mathcal{A}}(\alpha(p))$, $\bar{v}$ can maintain all the angle constraints given in $\bar{\mathcal{A}}$. However, this contradicts with the fact that $\bar{\mathbb{A}}$ is Z-weakly angle rigid, i.e., $\bar{v}$ must be the combination of p's translation, scaling and rotation along Z axis (corresponding to the existing six vectors in the kernel of $\bar{M}_{\mathcal{A}}(\alpha(p))$). Therefore, one has $\text{Rank}(\bar{M}_{\mathcal{A}}(\alpha(p)))=3N-6$. ■

In the 3D case, we also define $p=[p^{l\top},p^{f\top}]^\top$, where $p^l=[p_1^\top,p_2^\top]^\top\in\mathbb{R}^6$ and $p^f=[p_3^\top,\ldots,p_N^\top]^\top\in\mathbb{R}^{3N-6}$. The matrix $\bar{M}_{\mathcal{A}}(\alpha^*)$ can be correspondingly partitioned by $\bar{M}_{\mathcal{A}}(\alpha^*)=[\bar{M}^l_{\mathcal{A}}(\alpha^*),\bar{M}^f_{\mathcal{A}}(\alpha^*)]$ where $\bar{M}^l_{\mathcal{A}}(\alpha^*)\in\mathbb{R}^{6n^{\mathcal{A}}_{\triangle}\times6}$ and $\bar{M}^f_{\mathcal{A}}(\alpha^*)\in\mathbb{R}^{6n^{\mathcal{A}}_{\triangle}\times(3N-6)}$. Now, we define a new matrix

$$\bar{\mathcal{L}}(\alpha)=\bar{R}^\top_{\mathcal{A}}(\alpha)\bar{M}_{\mathcal{A}}(\alpha)=\begin{bmatrix}\bar{\mathcal{L}}_{ll} & \bar{\mathcal{L}}_{lf}\\ \bar{\mathcal{L}}_{fl} & \bar{\mathcal{L}}_{ff}\end{bmatrix}\in\mathbb{R}^{3N\times3N} \qquad (39)$$

where $\bar{\mathcal{L}}_{ll}=(\bar{M}^l_{\mathcal{A}})^\top\bar{M}^l_{\mathcal{A}}\in\mathbb{R}^{6\times6}$, $\bar{\mathcal{L}}_{lf}=(\bar{M}^l_{\mathcal{A}})^\top\bar{M}^f_{\mathcal{A}}\in\mathbb{R}^{6\times(3N-6)}$, $\bar{\mathcal{L}}_{fl}=(\bar{M}^f_{\mathcal{A}})^\top\bar{M}^l_{\mathcal{A}}\in\mathbb{R}^{(3N-6)\times6}$, and $\bar{\mathcal{L}}_{ff}=(\bar{M}^f_{\mathcal{A}})^\top\bar{M}^f_{\mathcal{A}}\in\mathbb{R}^{(3N-6)\times(3N-6)}$.

Lemma 3: If $\bar{\mathbb{A}}^*(\mathcal{V},\bar{\mathcal{A}},p^*)$ in 3D is Z-weakly angle rigid and Assumption 2 holds, then $\bar{\mathcal{L}}_{fl}(\alpha^*)p^{l*}+\bar{\mathcal{L}}_{ff}(\alpha^*)p^{f*}=0$, and the matrix $\bar{\mathcal{L}}_{ff}(\alpha^*)$ is positive definite.

Proof: Firstly, according to (33) and Theorem 3, one directly has $\bar{\mathcal{L}}_{fl}(\alpha^*)p^l*+\bar{\mathcal{L}}_{ff}(\alpha^*)p^{f*}=0$. The proof of $\bar{\mathcal{L}}_{ff}(\alpha^*)$ being positive definite can be obtained by following the same line as the proof of Lemma 1. ■

C. Formation Maneuvering Algorithm Design in 3D

Consider that the desired 3D formation is specified by a desired Z-weakly angle rigid angularity $\bar{\mathbb{A}}(\mathcal{V},\bar{\mathcal{A}},p^*)$. Using Lemma 3, the desired positions and velocities of the followers can be written by $p^{f*}(t):=-\bar{\mathcal{L}}^{-1}_{ff}(\alpha^*)\bar{\mathcal{L}}_{fl}(\alpha^*)p^l(t)$, $v^{f*}(t):=-\bar{\mathcal{L}}^{-1}_{ff}(\alpha^*)\bar{\mathcal{L}}_{fl}(\alpha^*)v^l(t)$. Therefore, the nonlinear control objective (6) in this 3D case can also be transformed into the linear form (14).

For the case that the two leaders have the same constant velocity, i.e., $\ddot{p}^l(t)=0$, we design the formation maneuvering formation law for the followers in the compact form as

$$\begin{aligned}u_f(t)=&-k_p\left[\bar{\mathcal{L}}_{ff}(\alpha^*)p^f(t)+\bar{\mathcal{L}}_{fl}(\alpha^*)p^l(t)\right]\\ &-k_v\left[\bar{\mathcal{L}}_{ff}(\alpha^*)v_f(t)+\bar{\mathcal{L}}_{fl}(\alpha^*)v_l(t)\right]\end{aligned} \qquad (40)$$

where $u_f(t)=[u_3^\top,\ldots,u_N^\top]^\top\in\mathbb{R}^{3N-6}$. According to (39), the component form of the formation maneuvering law (40) can be similarly obtained following (16). Now, we have the main results.

Theorem 4: Suppose Assumption 2 holds. If the desired 3D angularity $\bar{\mathbb{A}}^*(\mathcal{V},\bar{\mathcal{A}},p^*)$ is Z-weakly angle rigid and the two leaders have the same constant velocity, then under (40), the maneuvering objective (14) is globally achieved.

Proof: Substituting the control law (40) into (5), one has

$$\ddot{\tilde{p}}_f(t)+k_v\bar{\mathcal{L}}_{ff}(\alpha^*)\dot{\tilde{p}}_f(t)+k_p\bar{\mathcal{L}}_{ff}(\alpha^*)\tilde{p}^f(t)=0 \qquad (41)$$

where we used $\ddot{p}^l(t)=0$. Since (41) is a linear system, $\bar{\mathcal{L}}_{ff}$ is positive definite and $k_p>0,k_v>0$, $\tilde{p}(t)$ and $\tilde{v}_f(t)=\dot{\tilde{p}}_f(t)$ will globally and exponentially converge to 0. ■

Note that for the case where the leaders have time-varying moving velocities, one can design a similar formation algorithm as (20) to achieve the desired maneuvering. Now, we provide a simple example to illustrate the controller (40).

Example 2: Consider agents 1 and 2 as the leaders, agents 3 and 4 as the followers and $S_{\triangle1234}\in\mathcal{A}$. Following the definitions given after (16), the control law for agent 3 can be written as:

$$\begin{aligned}u_3=&-k_p(A_3^{\triangle1234}(\alpha^*))^\top[A_1^{\triangle1234}(\alpha^*)(p_1-p_3)\\ &-A_2^{\triangle1234}(\alpha^*)(p_2-p_3)-A_4^{\triangle1234}(\alpha^*)(p_4-p_3)]\\ &-k_v(A_3^{\triangle1234}(\alpha^*))^\top[A_1^{\triangle1234}(\alpha^*)(v_1-v_3)\\ &-A_2^{\triangle1234}(\alpha^*)(v_2-v_3)-A_4^{\triangle1234}(\alpha^*)(v_4-v_3)]\end{aligned} \qquad (42)$$

where $A_3^{\triangle1234}(\alpha^*)$ follows the definition given in (31). ■

Remark 3: Although the angle-displacement and affine formation maneuvering approaches (see e.g., [5], [8], [28], [29]) also enable the maneuvering motions of simultaneous translation, rotation and scaling, the number of leaders should be at least 4 in [8], and at least 3 for 2D maneuvering and at least 4 for 3D maneuvering in [5] and [29]. Compared with these available maneuvering approaches, both of our proposed 2D and 3D maneuvering laws only need 2 leaders. Although the proposed bearing-constrained formation maneuvering law in [13] also only needs at least 2 leaders, it requires all the agents' coordinate frames to have the same orientation. Compared with [24] and [27], no inter-agent communication is required in (15) and (40). A requirement of the 3D maneuvering algorithm (40) is that the desired formation should satisfy Assumption 2, which holds when p^*.

Remark 4: Due to the existence of two leaders, both $\mathcal{L}_{ff}(\alpha^*)$ in 2D and $\bar{\mathcal{L}}_{ff}(\alpha^*)$ in 3D are positive definite. However, if there are no leaders or only one leader, then $\mathcal{L}_{ff}$

and $\bar{\mathcal{L}}_{ff}$ are not positive definite and the current control design may not guarantee the convergence to the desired formation. This is because the null space of $\mathcal{L}(\alpha^*)$ and $\bar{\mathcal{L}}(\alpha^*)$ contains some vectors whose corresponding interior angles are not equal to the desired angles, such as $\sin\varphi(I_N \otimes B_1)p^*$ and $(1-\cos\varphi)(I_N \otimes B_2)p^*$ in $\bar{\mathcal{L}}(\alpha^*)$.

V. Extension to Lagrangian Dynamics and Minimum Number of Angle Constraints

A. Formation Maneuvering With Lagrangian Agent Dynamics

In practice, many mechanical systems can be modeled by Lagrangian dynamics, i.e.,

$$M_i(p_i)\ddot{p}_i + C_i(p_i,\dot{p}_i)\dot{p}_i + g_i(p_i) = \tau_i, \forall i \in \mathcal{V}_f \tag{43}$$

where i represents the ith agent, $p_i \in \mathbb{R}^d$ is the state, d denotes the degrees of freedom, $M_i(p_i)$ is symmetric and positive definite, $C_i(p_i,\dot{p}_i)$ is the Coriolis and centrifugal term, $g_i(p_i)$ is the gravitational term, and τ_i is the control input. Inspired by [38], one can design the following controller:

$$\tau_i = C_i(p_i,\dot{p}_i)\dot{p}_i + g_i(p_i) + M_i(p_i)u_i, \forall i \in \mathcal{V}_f \tag{44}$$

such that the model (43) can be transformed into a double-integrator dynamical model $\ddot{p}_i = u_i$, where we have used the fact that the inertial matrix $M_i(p_i)$ is always positive definite. Therefore, by substituting our proposed formation maneuvering laws (16) and (40) into (44), one can directly derive the formation maneuvering control law τ_f for the followers governed by Lagrangian agent dynamics.

B. Construction of Desired Angle Rigid Formations by Minimum Number of Angle Constraints

For the 2D case, since the sum of three interior angles in each triangle is constant, only two independent triplets exist in each $\mathcal{S}_{\triangle i_1 j_1 k_1}, (i_1, j_1, k_1) \in \mathcal{A}$. Therefore, to construct the desired angle rigid formation, one can select $2n-4$ angle constraints from $n-2$ triangles, which is the minimum number of constraints to guarantee triangular angle rigidity [23]. The combination form of these $n-2$ triangles can be constructed by using the Type-I vertex addition (Case 1) in [23].

For the 3D case, the minimum number of angle constraints in $\bar{\mathcal{A}}$ is $(4*3+3)*n_{\mathcal{A}}^{\triangle}$ since each tetrahedron has 4 triangular faces and three additional angle constraints with respect to the Z-axis. However, many of these angle constraints in $\bar{\mathcal{A}}$ are dependent. Instead, we now show how to use the minimum number of angle constraints, i.e., $3n-6$, to make $\bar{\mathbb{A}}$ Z-weakly angle rigid.

The first step uses three angle constraints: $\alpha^*_{312}, \alpha^*_{123}$ and the angle $\alpha^*_{(3Z,123)}$ between the ray $\overrightarrow{3Z}$ and the plane $\mathbb{P}_{123}$. As shown in Fig. 2, the first two angle constraints will make the interior angles of $\triangle 123$ unique, and the third angle constraint will allow $\triangle 123$ to only translate, scale, and rotate along the Z-axis. Subsequently, we use similar angle constraints to add agents $4,\ldots,N$ sequentially, see Fig. 2, of which each agent needs three angle constraints. Note that to distinguish $\triangle 123$ and the reflected $\triangle 1'2'3$, we require that $\alpha^*_{(3Z,123)}$ is the angle between $\overrightarrow{3Z}$ and the normal vector of $\overrightarrow{21} \times \overrightarrow{23}$. The same case applies to all the remaining vertices from 4 to N. Then, it can be verified that all the interior angles and the angles between the edges of those tetrahedra and Z-axis are uniquely determined. Therefore, only $3*(N-2)$ angle constraints are needed for this construction.

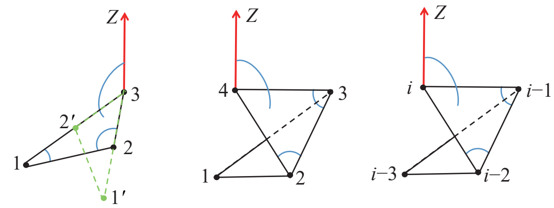

Fig. 2. Construct Z-weakly angle rigid formations by minimum number of angle constraints.

VI. Simulation Examples

This section presents two simulation examples with 4 followers to validate the effectiveness of the proposed formation maneuvering algorithms in 2D and 3D, respectively.

A. Formation Maneuvering in 2D Under Controller (15)

In this simulation, we consider agents 1 and 2 as leaders and agents 3 to 6 as followers. The agents' initial states are: $p_1(0)=[-1;-3], p_2(0)=[1;-3], p_3(0)=[0.4;-4.6], p_4(0)=[1.1;-5], p_5(0)=[-2;-3.7], p_6(0)=[2;-3.5], \dot{p}_1(0)=[0;1], \dot{p}_2(0)=[0;1], \dot{p}_3(0)=[0.1;-0.1], \dot{p}_4(0)=[0.2;0.1], \dot{p}_5(0)=[-0.1;-0.1], \dot{p}_6(0)=[0.4;-0.3]$. The desired formation is shown in Fig. 3. The control gains are $k_p=3, k_v=12$. We assume that the two leaders have the capability of autonomously maneuvering through a 2D unknown environment with obstacles, which can be achieved by using high-level motion planning algorithms. This simulation uses a polynomial form to plan the maneuvering parameters [29, Section V.B]. The agents' moving trajectories are shown in Fig. 4, which include translational, rotational and scaling maneuvering. The evolution of angle errors is shown in Fig. 5, which converge

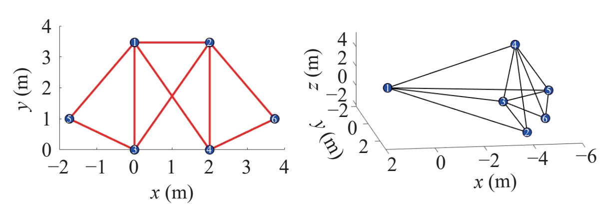

Fig. 3. The desired formations in 2D and 3D.

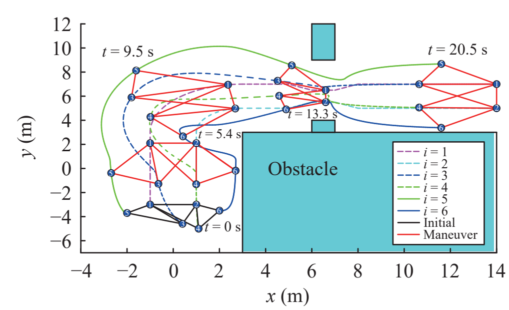

Fig. 4. Formation maneuvering trajectories in 2D under (15).

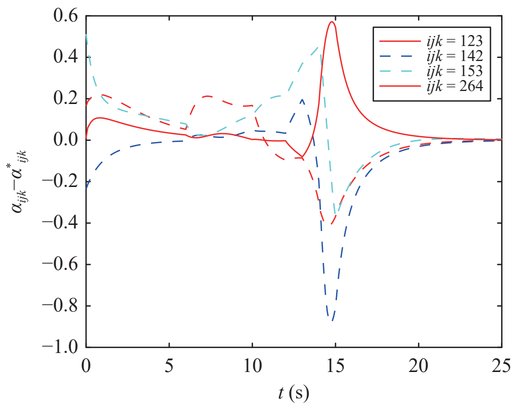

Fig. 5. Evolution of angle errors in 2D under (15).

to zero. The angle errors are observed to be nonzero during the maneuvering process because the leaders have time-varying velocity and the followers only execute (16).

B. Formation Maneuvering in 2D Under the Sliding Mode Controller (20)

In this simulation, we use the same initial states and desired formation as those in Section VI-A. The control gains are $k_p = 6, k_v = 1, \gamma_1 = 5, k_1 = 10$. The simulation results are shown in Figs. 6 and 7. Compared with Figs. 4 and 5, the convergence speed is faster and the overshoot is larger in Figs. 6 and 7.

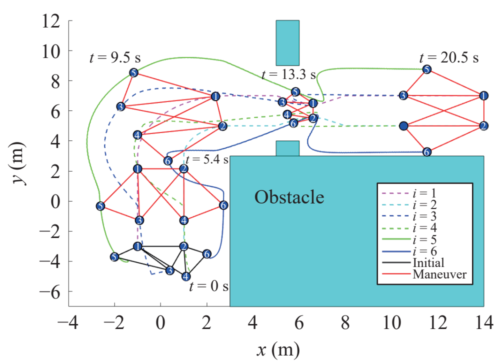

Fig. 6. Formation maneuvering trajectories in 2D under (20).

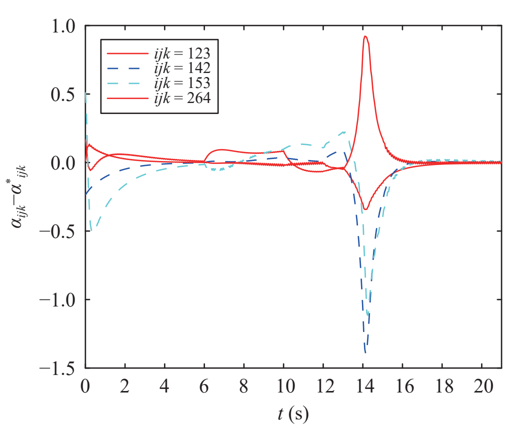

Fig. 7. Evolution of angle errors in 2D under (20).

C. Formation Maneuvering in 3D Under Controller (40)

We consider agents 1 and 2 as leaders and agents 3 to 6 as followers. The agents' initial states are: $p_1(0) = [-4+3\sqrt{3}; 0; 2.5/\sqrt{3}]$, $p_2(0) = [-4; 2; -2]$, $p_3(0) = [-4.4; -2.2; -2.42]$, $p_4(0) = [-4.4; 0; 6.01]$, $p_5(0) = [-5.5; 1.65; 2.2]$, $p_6(0) = [-4.95; 3.3; -0.55]$, $\dot{p}_1(0) = [0; 1.1; 0]$, $\dot{p}_2(0) = [0; 1.05; 0]$, $\dot{p}_3(0) = [0.1; 0.2; -0.1]$, $\dot{p}_4(0) = [0.2; -0.1; 0.1]$, $\dot{p}_5(0) = [0.2; -0.1; -0.2]$, $\dot{p}_6(0) = [0.1; 0.1; 0.1]$. The desired formation consists of three tetrahedra $\triangle$1234, $\triangle$1345, $\triangle$3456, which is shown in Fig. 3. The control gains are $k_p = 16, k_v = 6$. The agents' moving trajectories are shown in Fig. 8, which demonstrates the capability of simultaneous translational, rotational and scaling maneuvering. The evolution of angle errors is shown in Fig. 9.

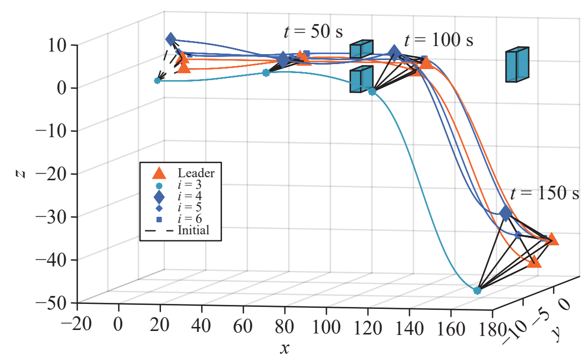

Fig. 8. Formation maneuvering trajectories in 3D under (40).

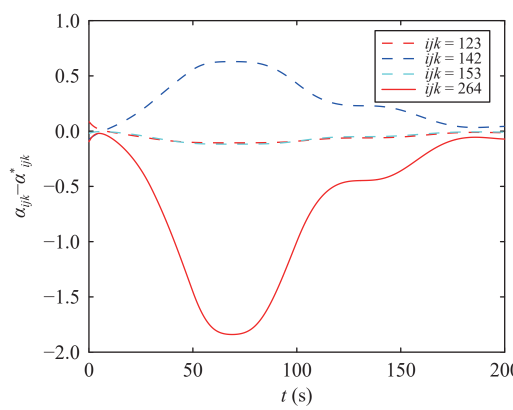

Fig. 9. Evolution of angle errors in 3D under (40).

VII. Conclusion

This paper has successfully achieved the maneuvering of angle rigid multi-agent formations in 2D and 3D with global convergence guarantees. For the 2D case, a formation algorithm has been designed to globally maneuver angle rigid formations using only relative position and velocity measurements in agents' local coordinate frames. For the 3D case, we have established angle-induced linear equations by assuming that all the agents have a common Z direction. Then, we have proposed a formation algorithm to maneuver Z-weakly angle rigid formations, where the number of each agent's required neighbors is reduced to three.

References

[1] H. S. Ahn, *Formation Control*. Cham, Germany: Springer, 2020.

[2] Y. G. Liu and G. Nejat, "Robotic urban search and rescue: A survey from the control perspective," *J. Intell. Robot. Syst.*, vol. 72, no. 2, pp. 147–165, Mar. 2013.

[3] J. Y. Hu, P. Bhowmick, I. Jang, F. Arvin, and A. Lanzon, "A decentralized cluster formation containment framework for multirobot systems," *IEEE Trans. Robot.*, vol. 37, no. 6, pp. 1936–1955, Dec. 2021.

[4] Q. Wang, Y. Z. Wang, and H. X. Zhang, "The formation control of multi-agent systems on a circle," *IEEE/CAA J. Autom. Sinica*, vol. 5, no. 1, pp. 148–154, Jan. 2016.

[5] S. Y. Zhao, "Affine formation maneuver control of multiagent systems," *IEEE Trans. Automat. Contr.*, vol. 63, no. 12, pp. 4140–4155, Dec. 2018.

[6] Z. M. Han, L. L. Wang, Z. Y. Lin, and R. H. Zheng, "Formation control with size scaling via a complex Laplacian-based approach," *IEEE Trans. Cybern.*, vol. 46, no. 10, pp. 2348–2359, Oct. 2015.

[7] L. M. Chen, H. G. De Marina, and M. Cao, "Maneuvering formations of mobile agents using designed mismatched angles," *IEEE Trans. Automat. Contr.*, vol. 67, no. 4, pp. 1655–1668, Apr. 2021.

[8] X. Fang, X. L. Li, and L. H. Xie, "Distributed formation maneuver control of multiagent systems over directed graphs," *IEEE Trans. Cybern.*, 2021, DOI: 10.1109/TCYB.2020.3044581.

[9] A. L. Yang, W. Naeem, and M. R. Fei, "Decentralised formation control and stability analysis for multi-vehicle cooperative manoeuvre," *IEEE/CAA J. Autom. Sinica*, vol. 1, no. 1, pp. 92–100, Jan. 2014.

[10] X. W. Dong and G. Q. Hu, "Time-varying formation control for general linear multi-agent systems with switching directed topologies," *Automatica*, vol. 73, pp. 47–55, Nov. 2016.

[11] A. Mondal, L. Behera, S. R. Sahoo, and A. Shukla, "A novel multi-agent formation control law with collision avoidance," *IEEE/CAA J. Autom. Sinica*, vol. 4, no. 3, pp. 558–568, Jul. 2017.

[12] Y. J. Lin, Z. Y. Lin, Z. Y. Sun, and B. D. O. Anderson, "A unified approach for finite-time global stabilization of affine, rigid, and translational formation," *IEEE Trans. Automat. Contr.*, vol. 67, no. 4, pp. 1869–1881, Apr. 2022.

[13] S. Y. Zhao and D. Zelazo, "Translational and scaling formation maneuver control via a bearing-based approach," *IEEE Trans. Contr. Netw. Syst.*, vol. 4, no. 3, pp. 429–438, Sep. 2017.

[14] Z. M. Han, K. X. Guo, L. H. Xie, and Z. Y. Lin, "Integrated relative localization and leader-follower formation control," *IEEE Trans. Automat. Contr*, vol. 64, no. 1, pp. 20–34, Jan. 2018.

[15] T. R. Han, Z. Y. Lin, R. H. Zheng, and M. Y. Fu, "A barycentric coordinate-based approach to formation control under directed and switching sensing graphs," *IEEE Trans. Cybern.*, vol. 48, no. 4, pp. 1202–1215, Apr. 2017.

[16] Z. X. Liu, Y. B. Li, F. Y. Wang, and Z. Q. Chen, "Reduced-order observer-based leader-following formation control for discrete-time linear multi-agent systems," *IEEE/CAA J. Autom. Sinica*, vol. 8, no. 10, pp. 1715–1723, Oct. 2020.

[17] Z. Y. Gao and G. Guo, "Fixed-time sliding mode formation control of AUVs based on a disturbance observer," *IEEE/CAA J. Autom. Sinica*, vol. 7, no. 2, pp. 539–545, Mar. 2020.

[18] H. G. De Marina, B. Jayawardhana, and M. Cao, "Distributed rotational and translational maneuvering of rigid formations and their applications," *IEEE Trans. Robot.*, vol. 32, no. 3, pp. 684–697, Jun. 2016.

[19] M. H. Trinh and H. S. Ahn, "Finite-time bearing-based maneuver of acyclic leader-follower formations," *IEEE Contr. Syst. Lett.*, vol. 6, pp. 1004–1009, Jun. 2021.

[20] X. L. Li, M. J. Er, G. H. Yang, and N. Wang, "Bearing-based formation manoeuvre control of nonholonomic multi-agent systems," *Int. J. Syst. Sci.*, vol. 50, no. 16, pp. 2993–3002, Nov. 2019.

[21] M. H. Trinh, Q. Van Tran, D. Van Vu, P. D. Nguyen, and H. S. Ahn, "Robust tracking control of bearing-constrained leader-follower formation," *Automatica*, vol. 131, p. 109733, Sep. 2021. DOI: 10.1016/j.automatica.2021.109733.

[22] S. Y. Zhao, Z. H. Li, and Z. T. Ding, "Bearing-only formation tracking control of multiagent systems," *IEEE Trans. Automat. Contr.*, vol. 64, no. 11, pp. 4541–4554, Nov. 2019.

[23] L. M. Chen, M. Cao, and C. J. Li, "Angle rigidity and its usage to stabilize multiagent formations in 2-D," *IEEE Trans. Automat. Contr.*, vol. 66, no. 8, pp. 3667–3681, Aug. 2021.

[24] G. S. Jing, G. F. Zhang, H. W. J. Lee, and L. Wang, "Angle-based shape determination theory of planar graphs with application to formation stabilization," *Automatica*, vol. 105, pp. 117–129, Jul. 2019.

[25] L. M. Chen, M. M. Shi, H. G. De Marina, and M. Cao, "Stabilizing and maneuvering angle rigid multi-agent formations with double-integrator agent dynamics," *IEEE Trans. Contr. Netw. Syst.*, 2022, DOI: 10.1109/TCNS.2022.3153885.

[26] J. Yang, X. M. Wang, S. Baldi, S. Singh, and S. Farì, "A software-in-the-loop implementation of adaptive formation control for fixed-wing UAVs," *IEEE/CAA J. Autom. Sinica*, vol. 6, no. 5, pp. 1230–1239, Sept. 2019.

[27] G. S. Jing and L. Wang, "Multiagent flocking with angle-based formation shape control," *IEEE Trans. Automat. Contr.*, vol. 65, no. 2, pp. 817–823, Feb. 2020.

[28] Z. Y. Lin, L. L. Wang, Z. Y. Chen, M. Y. Fu, and Z. M. Han, "Necessary and sufficient graphical conditions for affine formation control," *IEEE Trans. Automat. Contr.*, vol. 61, no. 10, pp. 2877–2891, Oct. 2016.

[29] L. M. Chen, J. Mei, C. J. Li, and G. F. Ma, "Distributed leader-follower affine formation maneuver control for high-order multiagent systems," *IEEE Trans.. Automat. Control*, vol. 65, no. 11, pp. 4941–4948, Nov. 2020.

[30] L. M. Chen and Z. Y. Sun, "Globally stabilizing triangularly angle rigid formations," *IEEE Trans. Autom. Contr.*, 2022, DOI: 10.1109/TAC.2022.3151567.

[31] R. Connelly, "Generic global rigidity," *Discrete Comput. Geom.*, vol. 33, no. 4, pp. 549–563, Apr. 2005.

[32] X. Fang, X. L. Li, and L. H. Xie, "Angle-displacement rigidity theory with application to distributed network localization," *IEEE Trans. Automat. Contr.*, vol. 66, no. 6, pp. 2574–2587, Jun. 2021.

[33] D. P. Yang, W. Ren, and X. D. Liu, "Fully distributed adaptive sliding-mode controller design for containment control of multiple Lagrangian systems," *Syst. Control Lett.*, vol. 72, pp. 44–52, Oct. 2014.

[34] L. G. Wu, J. X. Liu, S. Vazquez, and S. K. Mazumder, "Sliding mode control in power converters and drives: A review," *IEEE/CAA J. Autom. Sinica*, vol. 9, no. 3, pp. 392–406, Mar. 2022.

[35] M. C. Park, Z. Y. Sun, M. H. Trinh, B. D. O. Anderson, and H. S. Ahn, "Distance-based control of K4 formation with almost global convergence," in *Proc. IEEE 55th Conf. Decision and Control*, Las Vegas, USA, 2016, pp. 904–909.

[36] M. C. Park, Z. Y. Sun, B. D. O. Anderson, and H. S. Ahn, "Distance-based control of K_n formations in general space with almost global convergence," *IEEE Trans. Automat. Contr.*, vol. 63, no. 8, pp. 2678–2685, Aug. 2018.

[37] R. Kennedy and C. J. Taylor, "Network localization from relative bearing measurements," in *Proc. IEEE/RSJ Int. Conf. Intelligent Robots and Systems*, Chicago, USA, 2014, pp. 149–156.

[38] G. R. Duan, "High-order system approaches: I. Fully-actuated systems

and parametric designs," *Acta Autom. Sinica*, vol. 46, no. 7, pp. 1333–1345, Jul. 2020.

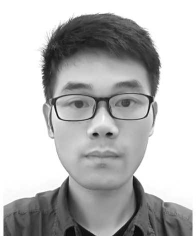

Liangming Chen received the B. E. degree in automation from Southwest Jiaotong University, in 2015. From 2015 to 2021, he has enrolled jointly in the Ph.D. program of systems and control in Harbin Institute of Technology, China and University of Groningen, the Netherlands. From 2021 to 2022, he has been a Research Fellow in the School of Mechanical and Aerospace Engineering, Nanyang Technological University, Singapore. His current research interests include formation control and distributed localization.

Zhiyun Lin (Senior Member, IEEE) received the Ph.D. degree in electrical and computer engineering from the University of Toronto, Canada, in 2005. He is currently a Full Professor in the Department of Electronic and Electrical Engineering, Southern University of Science and Technology. Preceding to this position, he was a Postdoctoral Research Associate (2005–2007) in the Department of Electrical and Computer Engineering, University of Toronto, then worked as a Research Professor (2007–2011) and Full Professor (2012–2017) at the College of Electrical Engineering, Zhejiang University, and served as the Director of the Artificial Intelligence Institute (2017–2021), Hangzhou Dianzi University. He has held many visiting professor appointments, including at Yale University (USA), The Australian National University (Australia), University of Groningen (The Netherlands), University of Cagliari (Italy), University of Newcastle (Australia), University of Technology Sydney (Australia), etc. His research interests focus on multi-agent systems, distributed artificial intelligence, autonomous systems and swarm robots, and cyber-physical systems. He was an Associate Editor for *IEEE Control Systems Letters*, *Hybrid Systems: Nonlinear Analysis*, etc. He is a Foreign Member of the Russian Academy of Engineering and a Fellow of IET.

Hector Garcia de Marina (Member, IEEE) received the M.Sc. degree in electronics engineering from the Complutense University of Madrid, Spain, in 2008, the M.Sc. degree in control engineering from the University of Alcala, Spain, in 2011, and the Ph.D. degree in systems and control from the University of Groningen, the Netherlands, in 2016. He held a postdoctoral position in the Ecole Nationale de l'Aviation Civile' in Toulouse from 2016 to 2018. From 2018 to 2020, he was an Assistant Professor at the Unmanned Aerial Systems Center, University of Southern Denmark. In 2020, he was a Research Fellow in the Complutense University of Madrid. Currently, he is a Research Fellow in the University of Granada under the Ramon y Cajal program. He is an Associate Editor for *IEEE Transactions on Robotics*. His research interests include the guidance navigation and control for autonomous robots, and multi-agent systems.

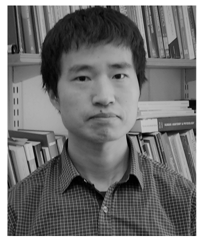

Zhiyong Sun received the Ph.D. degree from The Australian National University (ANU), Canberra ACT, Australia, in February 2017. He was a Research Fellow/Lecturer with the Research School of Engineering, ANU, from 2017 to 2018. From June 2018 to January 2020, he worked as a Postdoctoral Researcher at Department of Automatic Control, Lund University, Sweden. Since January 2020 he has been at Eindhoven University of Technology (TU/e), the Netherlands, as an Assistant Professor. His research interests include multi-agent systems, control of autonomous formations and distributed optimization.

Mir Feroskhan received first-class honors in aerospace engineering from Nanyang Technological University, Singapore, in 2011, and the Ph.D. degree in aerospace engineering from the Florida Institute of Technology, USA, in 2016. He is currently an Assistant Professor with the School of Mechanical and Aerospace Engineering at NTU. His research interests include nonlinear control systems, VTOL systems, drone design and development, flight dynamics and control, and aerial robotics.